Journal of Cellular Biochemistry 102:1432–1441 (2007)

Acetylation of Histone H4 in Complex Structural Transitions of Spermiogenic Chromatin

Kathryn Kurtz,[1] Fina Martínez-Soler,[1] Juan Ausió,[2] and Manel Chiva[1]*

[1]Department of Physiological Sciences II, Faculty of Medicine, University of Barcelona, Campus de Bellvitge, Barcelona, Spain
[2]Department of Biochemistry and Microbiology, University of Victoria, Victoria, British Columbia, Canada

Abstract In spermiogenic nuclei of the cephalopod mollusc *Sepia officinalis* histones are replaced by a precursor-protamine molecule, which is later converted into protamine. Simultaneously, spermiogenic chromatin undergoes a complex structural change. Somatic-like chromatin belonging to the earliest spermatid is progressively reorganized into: (a) granules of 20 nm diameter, (b) fibres of 30–35 nm, and (c) fibres of 40–50 nm. In the final phases of spermiogenesis these fibres of 40–50 nm join to form larger structures of condensed chromatin, and lastly, the uniformly packed chromatin in the sperm nucleus. Using specific antibodies for mono- and hyperacetylated forms of histone H4, in this work we show that the first structural remodelling of chromatin (from somatic-like organization into 20 nm granules) is given concomitantly with a massive mono-acetylation of H4 (acetylation in lysine 12), whereas the structural remodelling from 30–35 to 40–50 nm fibres is produced simultaneously with hyperacetylation of H4 and the nuclear removal of histones. J. Cell. Biochem. 102: 1432–1441, 2007.

Key words: H4 acetylation; spermiogenesis; chromatin structure

During the development of spermiogenesis in the major part of animal species, important changes occur in type and chemical modifications of nuclear proteins. This fact implies a series of progressive changes in the interaction between DNA and proteins, which bring about a continuous remodelling of chromatin structure, reaching to highly condensed chromatin in the ripe sperm nucleus.

In the most simple cases (Model: H → P), histones of the spermatidyl nucleus are directly replaced by a small and very basic protein designated as "protamine" which is the sole protein associated to DNA in the sperm nucleus. Spermiogenic protein transitions belonging to the H → P model are found among bony fish and birds, and they have been studied in the past by several authors (see Oliva and Dixon, 1991 for a review).

Nevertheless, evolution has generated enormous diversity in the spermiogenic processes of nuclear protein transitions and consequently, in the interaction of DNA and proteins, and also in the patterns of spermiogenic chromatin condensation [Chiva et al., 1995; Lewis et al., 2003, 2004; Harrison et al., 2005]. In the course of spermatogenesis of the cephalopod *Sepia officinalis*, nuclear histones are replaced by a basic protein of 77–78 amino acid residues during intermediate steps of spermiogenesis. This molecule (Protamine-precursor: Pp) is afterwards converted into mature protamine by an enzymatic deletion of its first 21 N-terminal residues [Martin-Ponthieu et al., 1991; Wouters-Tyrou et al., 1991]. We are studying the spermiogenesis of *S. officinalis* (Model: H → Pp → P) because it constitutes the level of complexity immediately superior to the model H → P.

In previous studies [Martínez-Soler et al., 2007a,b] we have analysed the progressive changes in the structure of *S. officinalis* spermiogenic chromatin, as well as the basic proteins associated with each particular type of chromatin. As can be observed in Figure 8, the

Grant sponsor: Ministerio de Educación y Ciencia; Grant number: BFU 2005-00123; Grant sponsor: Natural Sciences and Engineering Research Council; Grant number: OGP 0046399-02.

*Correspondence to: Manel Chiva, Pavelló de Govern 4° Planta, Hospitalet de Llobregat, Barcelona 8907, Spain.

Received 13 February 2007; Accepted 12 March 2007
DOI 10.1002/jcb.21365

chromatin of the earliest spermatid displays a somatic-like appearance, where histones are the main proteins interacting with DNA. In the next stages of spermiogenesis, the chromatin structure suffers a re-organization into granules of 20 nm diameter but continues containing histones as the main nuclear protein component. Afterwards, the chromatin is remodelled again into 30–35 nm diameter fibres that contain both histones and protamine-precursor. In more advanced steps, spermiogenic chromatin is reorganized into 40–50 nm fibres constituted by DNA associated with protamine-precursor molecules, and a very small amount of histones. In the final stages of spermiogenesis, the 40–50 nm fibres join to form aggregates of condensing chromatin displaying irregular sizes. These aggregates contain protamine.

The aim of this work is to study how the acetylation of histone H4 participates in the process of remodelling of *S. officinalis* spermiogenic chromatin by means to localize mono- and hyperacetylated forms of H4 in each particular chromatin structure.

In a previous work, Couppez et al. [1987] demonstrated that in the testis of cuttlefish, histone H4 is found partially in the non-acetylated form (41.4% of the whole gonadal H4), and partially in mono-, di-, tri- and tetra-acetylated forms (32.3, 18.0, 6.4 and 2%, respectively). The same study also established that in the male gonad of cuttlefish, acetylation of histone H4 is accomplished sequentially, in such a way that lysine 12 (K12) is the main site of acetylation in the monoacetylated form, whereas lysine 12 and 5 are found acetylated in diacetylated H4, and lysine 12, 5 and 16 are found acetylated in triacetylated H4.

Considering these previous results from Couppez et al. [1987], in the present work we have used a specific antibody against H4 acetylated on lysine 12 (anti-H4-acK12) in order to detect monoacetylation of histone H4, whereas hyperacetylation of H4 has been studied using the specific antibody against H4 acetylated on lysine 16 (anti-H4-acK16). We have analysed by electron immunomicroscopy the labelling of spermiogenic chromatin by each one of these two antibodies. The combination of results obtained shows that the remodelling of chromatin from somatic-like to 20 nm granular structures develops simultaneously with a massive monoacetylation of histone H4 (without removal of histones from the nucleus), whereas the remodelling from 30–35 nm into 40–50 nm fibres initiates with a hyperacetylation of H4 and finalizes with the removal of histones from the cell nucleus. These results complement the study of the main processes responsible for the structural transitions of chromatin in a complex model of spermiogenic nuclear protein changes ($H \rightarrow Pp \rightarrow P$) [Martínez-Soler et al., 2007a].

MATERIALS AND METHODS

Animals

Specimen of *S. officinalis* (a cephalopod mollusc) and *Trachinus draco* (an osteichthyan fish) were caught at the Mediterranean coast and identified by their morphological characters.

Antibodies

In this work four antibodies have been used: anti-acetyl lysine (Abcam, cat. # ab 21623), anti-H4 specifically acetylated in lysine 12 (anti-H4-acK12) (Upstate, catalogue # 07-329), whose antigen is the peptide GKGGA[acK]RHRKC, anti-H4 specifically acetylated in lysine 16 (Upstate, catalogue # 07-595), whose antigen is the peptide GKGLG[acK]GGAKRC, and an antibody against histone H2A (anti-H2A). The antibody anti-H4-acK16 presents low reactivity when used for electron microscopy immunolabelling, but displays a normal reactivity when used in Western blots obtained from denaturing electrophoretic gels. A possible explanation for this behaviour is that lysine 16 of histone H4 occupies a position very close to the globular core of molecule, and it may be only slightly accessible to the antibody when H4 protein is not completely denatured.

Whereas the three first antibodies are commercial (anti-H4-acK12 and anti-H4-acK16 from Upstate, and anti-acetyl lysine from Abcam), anti-H2A antibody was generated from H2A histone purified from calf thymus according to the method of Johns [1967], and submitted to controls explained in Martínez-Soler et al. [2007a].

Nuclear Proteins

Nuclei were obtained from testis of *S. officinalis* as in Saperas et al. [2006]. Briefly: Gonads of *S. officinalis* and *T. draco* were homogenized in buffer A (0.25 M sucrose, 5 mM $CaCl_2$, 10 mM Tris/HCl pH7.4, 10 mM benzamidine chloride),

filtered and centrifuged. Pellets were homogenized and centrifuged again with buffer A containing 0.25% Triton X-100 and the complete procedure was repeated two more times. The last sediment (purified nuclei) was washed with 10 mM Tris pH 7.4, and basic proteins extracted by 5 volumes of 0.4 N HCl, cleared by centrifugation, precipitated and washed with acetone [Saperas et al., 2006].

Electrophoretic Analysis of Proteins

Two-dimensional electrophoresis was performed according to the procedure described by Dimitrov and Wolffe [1997] with minor variations. In the first dimension, the histones were separated in 6 M urea, 6 mM Triton X-100 in 15% acrylamide. A single lane of electrophoresed proteins was excised from the gel of the first dimension, and incubated briefly in 8 M urea containing methylene green as a running marker. This first dimension was then laid on top of a second dimension gel, which contained two portions: a running gel, overlain with a concentrating gel. The running gel contained 6 M urea, 0.9 M acetic acid, and 0.6 mM Triton X-100. The overlaying concentrating gel was about 2 cm thick, containing the same components of the running gel, but with the Triton X-100 detergent omitted. The gel was run at 100 V until the methylene green marker ran off the bottom of the gel.

Protein Acetylation Analysis by Western Blots

Following electrophoresis of the second dimension, the gel was transferred to a PVDF membrane and probed for the presence of acetylated histones, using anti-acetyl lysine (Abcam), anti-H4-acK12 (Upstate), or anti-H4-acK16 (Upstate). The antibodies recognizing specific acetylated lysine residues on H4 were diluted 1:2,000 in PBS containing 5% powdered skim milk, and anti-acetyl lysine was prepared in PBS containing 2.5% foetal calf serum and 2.5% powdered skim, at a dilution of 1:250, and incubated at 4°C overnight with shaking. Antibody recognition of acetylated residues by all antibodies mentioned was detected using an HRP conjugated goat anti-rabbit secondary antibody diluted 1:3,000 in PBS containing 5% powdered skim milk, and incubated for 1.5 h at room temperature with agitation. HRP detection was performed using an ECL reagent (Amersham). PVDF membranes were stained with Ponceau-S (Sigma) and protein spots or bands on the film were unambiguously identified by superposition, and quantified in an automatic system (Phoretix 1D).

Electron Microscopy and Immunomicroscopy

Small sections of gonad have been fixed and embedded in Spur resin for conventional electron microscopy, or in Lowicryl resin for immunomicroscopy experiments [Giménez-Bonafé et al., 2002].

For electron immunomicroscopy examination, we have tried out a variety of blocking conditions and dilutions of both primary and secondary antibodies. The following working conditions are those which have been selected.

Anti-acetyl lysine (Abcam). The nickel grids containing the ultrafine sections of gonadal or epididymal tissue were blocked for 30 min in 0.1 M PBS pH 8.5 containing 2% powdered skim milk, 2% normal goat serum, and 20 mM glycine. The antibody was diluted 1:25 and 1:100 in the same blocking solution, with the glycine omitted. Tissue samples treated with anti-H4-acK16 were blocked for 30 min in 0.1 M PBS pH 8.5 containing 1.5% of each powdered skim milk and normal goat serum with 20 mM glycine. The primary antibody was diluted 1:100 in this same solution, with the glycine omitted. Anti-H4-acK12 and anti-H2A were treated with the same conditions as those used for anti-H4-acK16. All primary antibody incubations lasted for 2 h. The secondary antibody used for all treated samples was a 15 nm colloidal gold conjugated goat anti-rabbit antibody, diluted 1:25 in the same solution which was used to dilute the respective primary antibody, and applied for 1 h. All treatments were performed at room temperature.

Under these circumstances the controls treated exclusively with secondary antibody produced minimal or no labelling in spermatic nuclei, and the general background conditions were the lowest observed. These are the only variations of the general method described previously [Giménez-Bonafé et al., 2002] for electron immunomicroscopy.

RESULTS

General Acetylation of Histone H4 in Testis of *S. officinalis*

To study the behaviour of antibodies anti-H4-acK12/-acK16 by electron microscopy, and in order to verify the agreement of our results with

those described by Couppez et al. [1987], we have re-examined the appearance and the proportions of H4 acetylated populations in testis of *S. officinalis*.

It is necessary to point out that the relative ratios among different stages of spermiogenic cells change depending on the degree of maturity of *S. officinalis* testis. Advanced steps of spermiogenic cells (which may contain a higher degree of histone acetylation) are more frequent in ripe gonads than in those that are immature [Martínez-Soler et al., 2007b]. For these reasons, the relative proportion of H4 acetylated forms described by Couppez et al. [1987] should be considered only as an approximate, but not absolute, value.

Figure 1A displays a two-dimensional electrophoretic development of proteins extracted from whole gonadal nuclei prepared from a mature testis of *S. officinalis*. The electrophoresis has been performed in 6 mM Triton/6 M urea (first dimension) and 0.6 mM Triton/6 M urea for the second dimension, and has been stained with Coomassie blue. Under these conditions, histone H4 and its acetylated forms show a good resolution without any contamination of other protein spots, because they separate from the diagonal formed by the major part of proteins [Dimitrov and Wolffe, 1997]. The zone corresponding to histone H4 and acetylated H4 appears magnified in Figure 1B. Stained by Coomassie blue, the non-acetylated (0 in Fig. 1B), mono-acetylated (1 in Fig. 1B) and di-acetylated H4 (2 in Fig. 1B) appear clearly in the gel with a decreasing intensity, but tri- and tetra-acetylated are minor fractions of histone H4 and are not detected by Coomassie blue at the protein concentration used for this electrophoresis. The proportion between non-, mono- and di-acetylated H4 estimated from Figure 1B is respectively 5/2/1. This value is roughly coincident with ratio given by Couppez et al. [1987].

General acetylated forms of H4 histone have been revealed by Western blot of two-dimensional electrophoresis using the antibody anti-acetyl lysine, which unespecifically recognizes acetylated proteins. In Figure 1C one can observe that the intensity of labelling for H4 acetylated forms decreases from mono- to tetra-acetyl H4. However, the relative intensity of each population cannot be measured in a reliable way in these blots, due to overlapping of spots.

Detection of H4 Acetylation by Western Blot Using the Antibodies Anti-H4-acK12 and Anti-H4-acK16

Figure 2 shows the cross-reaction between antibody anti-H4-acK12 and the whole testicular proteins of *S. officinalis* (s1, s2 in Fig. 2), compared with a control (t1, t2) obtained from *T. draco*, a bony fish which accumulates hyperacetylation of H4 during spermiogenesis (unpublished results). Mono-acetylated H4 of *S. officinalis* clearly appears as the major acetylated form, while the intensity of the next acetylated levels of H4 decrease progressively. The approximate ratio between acetylated populations of H4 has been evaluated from the intensity of bands appearing in lane s1 (Fig. 2). The value obtained is 4/2.5/1 for mono-, di- and tri-acetylated H4, respectively. Tetra-acetylated H4 appears always as a very minor fraction in *S. officinalis* testis (see Discussion)

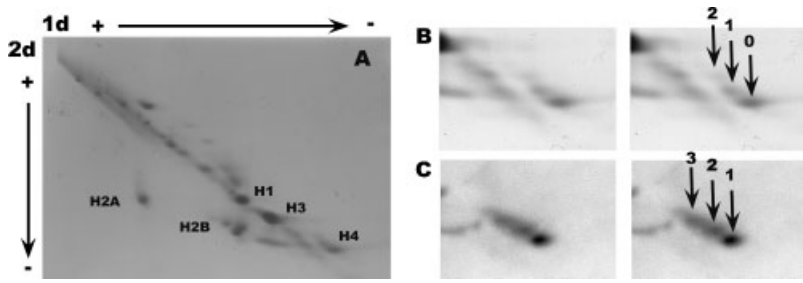

Fig. 1. Immunodetection of acetylated forms of H4 by anti-acetyl lysine antibody in *S. officinalis* male gonad. **A**: Two-dimensional electrophoresis of whole proteins extracted from testicular nuclei of *S. officinalis* by 0.4 N HCl. First dimension: 6 mM Triton/6 M urea; second dimension 0.6 mM Triton/6 M urea. **B**: Magnification of zone corresponding to H4 (0) and acetylated forms (1: mono-acetylated H4; 2: di-acetylated H4). **C**: Western blot and immunodetection of acetylated H4 by the antibody anti-acetyl lysine (1: mono-; 2: di-, 3: tri-acetylated H4).

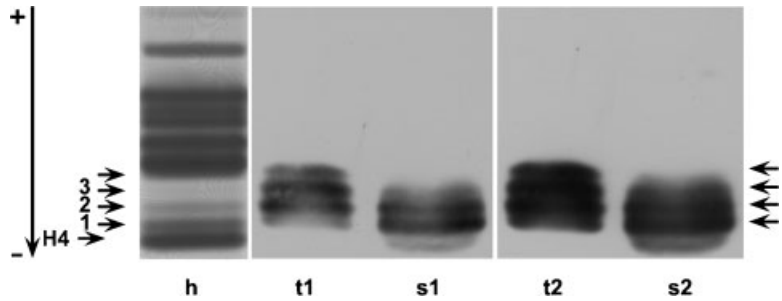

Fig. 2. Immunodetection of acetylated forms of H4 by anti-H4-acK12 in testis of *S. officinalis*. **Lane h**: Acetic acid/urea electrophoresis of testicular histones of *S. officinalis*. **Lanes s1** and **s2**: Immunodetection of acetylated H4 by anti-H4-acK12 (s2 identical to s1 with developing increased). **Lanes t1** and **t2**: Forms from mono- to tetra-acetylated H4 obtained from intermediate spermatidyl nuclei of *Trachinus draco*. In this species of bony fish all the gonadal H4 accumulates hyperacetylation before to be replacement by protamine (1, 2, 3: mono-, di-, and tri-acetylated H4).

and does not appear clearly in the blots performed in this work.

The values obtained here are in agreement with those obtained by Couppez et al. [1987] and with the ratios evaluated from Figure 1B. A more important point is that this coincidence in results corroborates that lysine K12 is the first lysine to be acetylated in gonadal H4 molecules. If this were not the case, the proportion found using anti-H4-acK12 would differ from the general proportion of acetylated forms.

The cross-reaction of antibody anti-H4-acK16 with acetylated H4 gonadal forms is displayed in Figure 3. In this case the intensity of labelling of mono-, di- and tri-acetylated forms is similar (1/1/1, respectively) (Fig. 3, lane s). This ratio is not a complete contradiction to the results of Couppez et al. [1987], according to which lysine 16 is the third lysine to be acetylated in gonadal H4, but that a small proportion of monoacetylated H4 also exists whose site of acetylation is lysine 16. Our results also show that a proportion of mono- and di-acetylated H4 is acetylated on lysine 16. Nevertheless, if we take into consideration that the absolute level of tri-acetylated H4 is very low compared to mono- and di-acetylated H4 (Figs. 1B and 2), we should conclude that antibody anti-H4-acK16 reacts preferentially (not exclusively) with tri-acetylated H4.

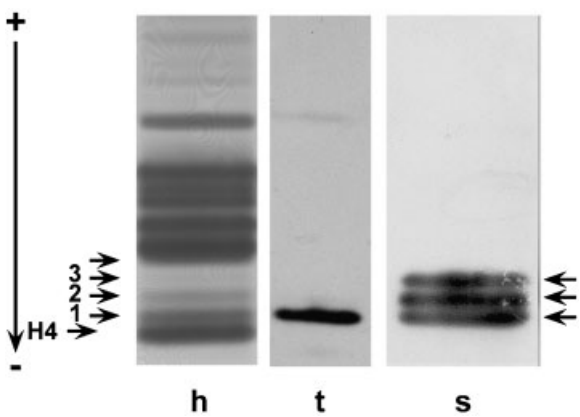

Fig. 3. Immunodetection of acetylated forms of H4 by anti-H4-acK16 in testis of *S. officinalis*. **Lane h**: Acetic acid/urea electrophoresis of testicular histones of *S. officinalis*. **Lane s**: Immunodetection of acetylated H4 by the antibody anti-H4-acK16. **Lane t**: Control of mono-acetylated H4 obtained from *T. draco* (1, 2, 3: mono-, di-, and tri-acetylated H4).

Immunolabelling of *S. officinalis* Spermiogenic Chromatin

We have assayed a series of working conditions to observe by electron microscopy the antibody labelling of *S. officinalis* spermiogenic chromatin. We have chosen the specific conditions in which the nuclear labelling is maximum, whereas extranuclear background is maintained in a practically null level. All the following results are presented at the same conditions (described in Materials and Methods).

The labelling of different phases of *S. officinalis* spermiogenic chromatin by the antibody anti-H4-acK12 is shown in Figure 4. Earliest spermatids contain somatic-like chromatin that shows a very low degree of cross-reaction with the antibody (Fig. 4A). The first structural remodelling of chromatin drives to granular structures of 20 nm which are homogeneously distributed in the cell nucleus. This chromatin strongly reacts with anti-H4-acK12 (Fig. 4B). Chromatin organized in 30–35 nm fibres (next structure in spermiogenesis) reacts also intensely with this antibody (Fig. 4C), where the

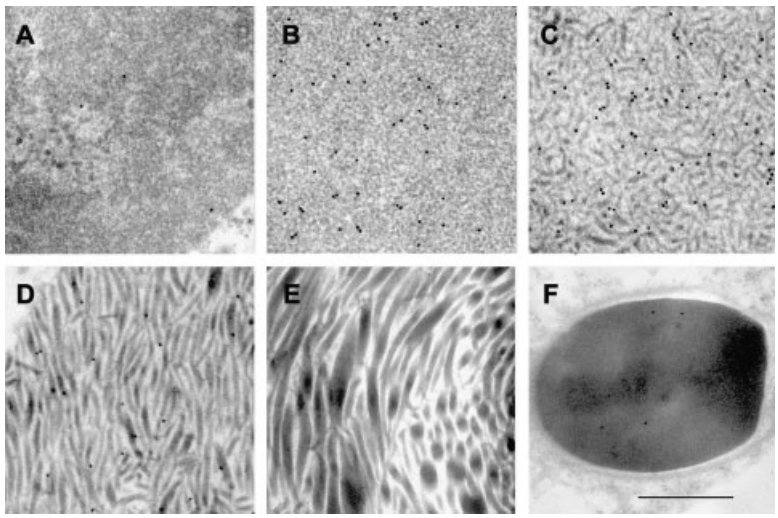

Fig. 4. Immunogold labelling of *S. officinalis* spermiogenic chromatin structures by anti-H4-acK12. **A**: Somatic-like chromatin; **B**: 20 nm granular chromatin; **C**: 30–35 nm fibrillar chromatin; **D**: 40–50 nm fibrillar chromatin; **E**: Advanced step of chromatin condensation; **F**: Chromatin fully condensed belonging to a testicular spermatozoon. Bar: 500 nm for (A)–(E), and 1,000 nm for (F).

labelling is even slightly superior than in 20 nm granular chromatin. The reaction with anti-H4-acK12 appears remarkably diminished in the next spermiogenic chromatin structure (40–50 nm fibres) (Fig. 4D), and at the final phases of condensation (Fig. 4E,F) the reaction with the antibody completely disappears.

We have performed the same observations using the antibody anti-acetyl lysine. The results (not shown) are qualitatively identical, but the level of labelling is superior, since in this case all acetylated proteins participated in the reaction.

The chromatin labelling by antibody anti-H4-acK16 is always weak when compared with the former (see Materials and Methods). In Figure 5A,B one can observe that both somatic-like chromatin from earliest spermatids, as well as granular chromatin do not react significantly with anti-H4-acK16. Nuclei with chromatin organized in 30–35 nm fibres exhibit the highest degree of antibody labelling (Fig. 5C,D). In the following spermiogenic stage, the labelling of 40–50 nm chromatin fibres diminishes with respect 30–35 nm fibres (Fig. 5D), and in the next stages (Fig. 5E,F) the labelling is null.

To understand correctly the preceding results observed, using the same conditions we studied the cross-reaction of spermiogenic chromatin of *S. officinalis* with an anti-H2A antibody, elicited from histone H2A purified from calf thymus. This part serves here as a control of the presence of histones in each one of the particular structures of spermiogenic chromatin. The observations (Fig. 6) show that in somatic-like chromatin of earliest spermatids, the reaction with anti-H2A is given mainly in the zone occupied by heterochromatin, were density of nucleosomes is high (Fig. 6A). The signal found in granular chromatin is similar or slightly superior (Fig. 6B), whereas in 30–35 nm fibres, labelling returns to the initial values (Fig. 6C). Labelling remarkably diminishes during the remodelling from 30–35 to 40–50 nm fibres (Fig. 6D), and disappears finally in the last steps of condensation. A semiquantitative comparison of immunogold labelling by the different antibodies used is represented in Figure 7.

DISCUSSION

In spermiogenesis belonging to the model H → P, the transition of nuclear proteins is relatively simple. Histones of early spermatids become hyperacetylated in the intermediate stages of spermiogenesis and are replaced by phosphorylated protamine. Afterwards, in the last phases of spermiogenesis, protamine suffers dephosphorylation and remains in the sperm nuclei maintaining DNA in a highly packed state [Subirana, 1983; Christensen et al., 1984]. The changes of DNA-interacting proteins induce also relatively simple transitions in chromatin structure (condensation pattern). The pattern of condensation starts from somatic-like chromatin (first spermiogenic

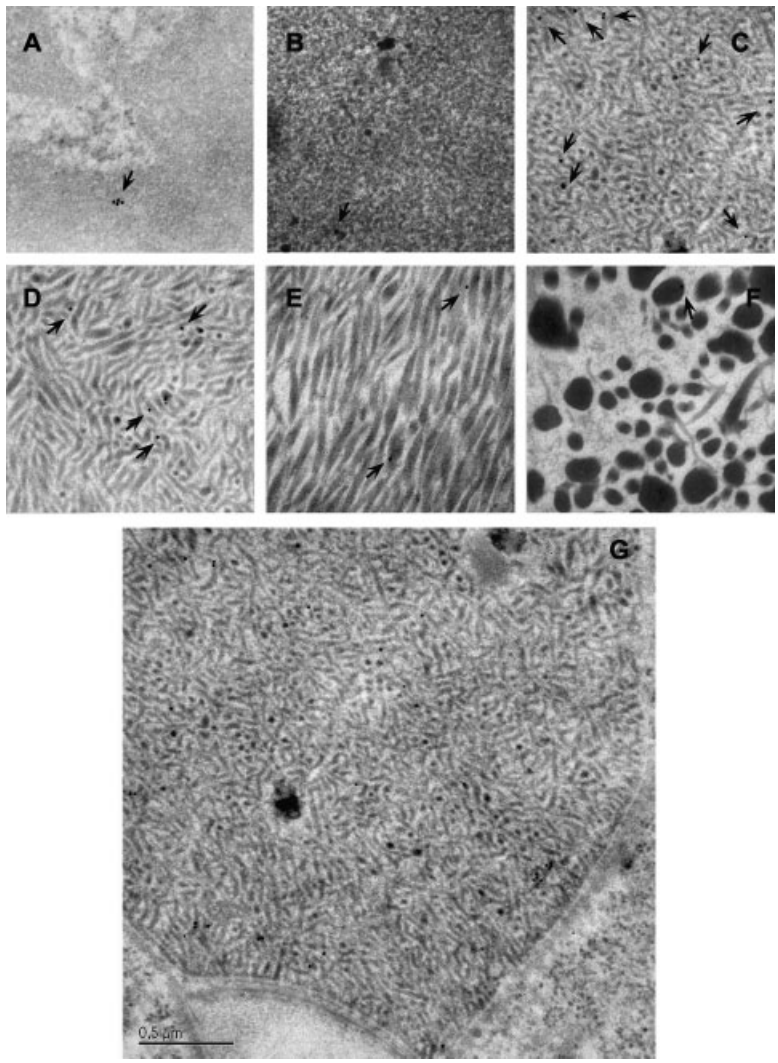

Fig. 5. Immunogold labelling of *S. officinalis* spermiogenic chromatin structures by anti-H4-acK16. **A**: Somatic-like chromatin; **B**: 20 nm granular chromatin; **C**,**G**: 30–35 nm fibrillar chromatin; **D**: 40–50 nm fibrillar chromatin; **E**,**F**: Advanced steps of chromatin condensation. Bar: 500 nm for all images.

stages) evolving to granular chromatin (intermediate stages), and finally to condensed chromatin by protamine [Saperas et al., 1993].

Spermiogenesis of *S. officinalis* belongs to a more complex model of nuclear protein transitions (H → Pp → P). In these cases an additional protein appears between histones and mature protamine. This protein is a precursor of the protamine molecule [Wouters-Tyrou et al., 1991]. This fact (relatively simple at the molecular level) produces a remarkable increase in complexity in the spermiogenic pattern of chromatin condensation; that is, the number of different structures adopted by chromatin during spermiogenesis is higher than would be expected. In Figure 8 appears a selection of main steps in the pattern of condensation of *S. officinalis* spermiogenic chromatin. This pattern comprises three structural remodellings (Fig. 8A–D: somatic-like chromatin → 20 nm granules → 30–35 nm fibres → 40–50 nm fibres), a final period where the 40–50 nm fibres are joining to form larger structures, and lastly, uniformly packed chromatin (Fig. 8E,F). In a previous work [Martínez-Soler et al. 2007a] we showed that the endowment of histones associated to chromatin remains complete until 30–35 nm fibres, and drastically diminishes in fibres of 40–50 nm. Simultaneously, protamine-precursor (Pp) appears

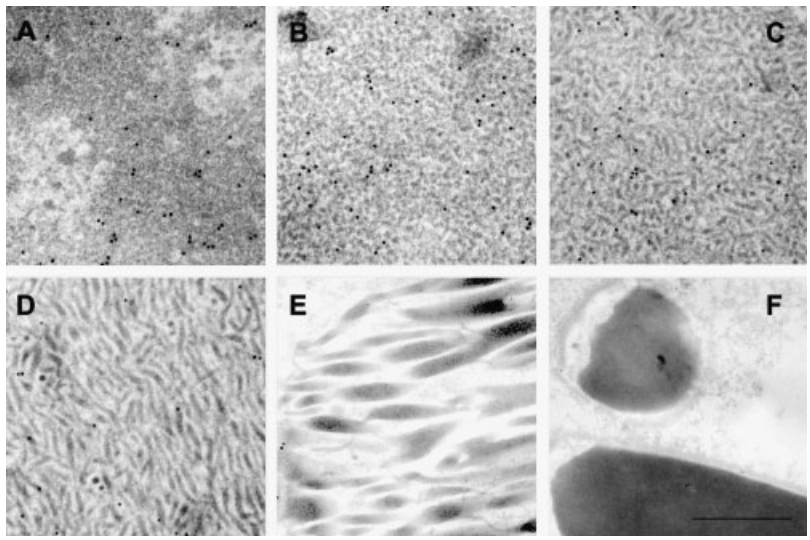

Fig. 6. Immunogold labelling of *S. officinalis* spermiogenic chromatin structures by anti-H2A. **A**: Somatic-like chromatin; **B**: 20 nm granular chromatin; **C**: 30–35 nm fibrillar chromatin; **D**: 40–50 nm fibrillar chromatin; **E**: Advanced step of chromatin condensation; **F**: Chromatin fully condensed belonging to a testicular spermatozoon. Bar: 500 nm for (A)–(E), and 1,000 nm for (F).

swiftly in chromatin organized into 30–35 nm fibres and is converted into the phosphorylated protamine in the final phases of spermiogenesis.

In the present work we analyse the presence of acetylated forms of histone H4 in the pattern of *S. officinalis* chromatin condensation using specific antibodies for acetyl-H4 lysine12, and acetyl-H4 lysine 16. The results (discussed next) have been incorporated in Figure 8.

During the first remodelling (somatic-like → 20 nm granules) the labelling with antibody anti-H4-acK12 suffers an important increase, but we have not detected any significant labelling with anti-H4-acK16. If we consider that these antibodies preferably react with mono-acetylated H4 (anti-H4-acK12), and tri-acetylated H4 (anti-H4-acK16), we should conclude that first step of chromatin remodelling develops simultaneously with a massive mono-acetylation of histone H4 at lysine 12. To our knowledge, this is the first report of global histone H4 acetylation [Calestagne-Morelli and Ausió, 2006] affecting only this residue. The size of granules (20 nm in diameter) allows a packing

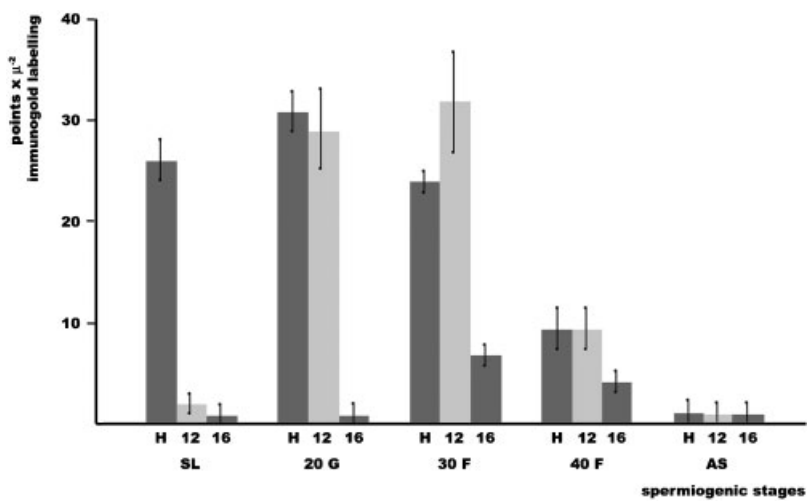

Fig. 7. Immunogold labelling (particles/μm^2) by antibodies anti-H2A (H), anti-H4-acK12 (12), and anti-H4-acK16 (16) at different stages of spermiogenic chromatin of *S. officinalis*. SL: Somatic-like chromatin. 20G: 20 nm granular chromatin. 30F: 30–35 nm fibres. 40F: 40–50 nm fibres. AS: advanced stages.

of 4–6 nucleosomes. We speculate that monoacetylation of H4 at lysine 12 (and other histones not considered here) may favour an ordered gathering of small groups of nucleosomes, although this point deserves to be studied with more detail. The next remodelling drives to 30–35 nm fibres that contain an interesting composition of proteins. First, the level of histones in this chromatin (detected by antibody anti-H2A independently in this work, and in Martínez-Soler et al. [2007b]) seems to be practically the same as that which is found in the somatic chromatin. Second, the level of acetylation/hyperacetylation of histone H4 is the largest found among all spermiogenic chromatin stages. Third, this chromatin also contains the complete endowment of protamine-precursor molecules [see Martínez-Soler et al., 2007b]. The structure of 30–35 nm fibres should be related to a dynamical equilibrium of the reaction

$$\mathrm{Pp} + \mathrm{DNA} - \mathrm{acHist} \leftrightarrow \mathrm{Pp} - \mathrm{DNA} - \mathrm{acHist} \leftrightarrow \mathrm{Pp} - \mathrm{DNA} + \mathrm{acHist}$$

in which, nucleosomes will leave DNA when histone acetylation reaches a threshold. The threshold value seems to be tetra-acetylated status since tetra-acetylated form of H4 practically cannot be detected in *S. officinalis* testicular nuclei (see Figs. 1–3). Displacement of the reaction to the right is related to structural chromatin remodelling. In 40–50 nm fibres there are residues of hyperacetylated histones (compare labelling of anti-H4-acK12 and anti-H4-acK16 with anti-H2A in Figs. 4–6), but the main DNA-interacting protein is largely the protamine-precursor [Martínez-Soler et al., 2007b]).

In the last phases of spermiogenesis (condensation phases, Fig. 7D–F) histones have completely disappeared and chromatin associated proteins are protamine-precursor, protamine and their dephosphorylated forms [Martínez-Soler et al., 2007b]. Therefore, the final condensation of chromatin is given by the

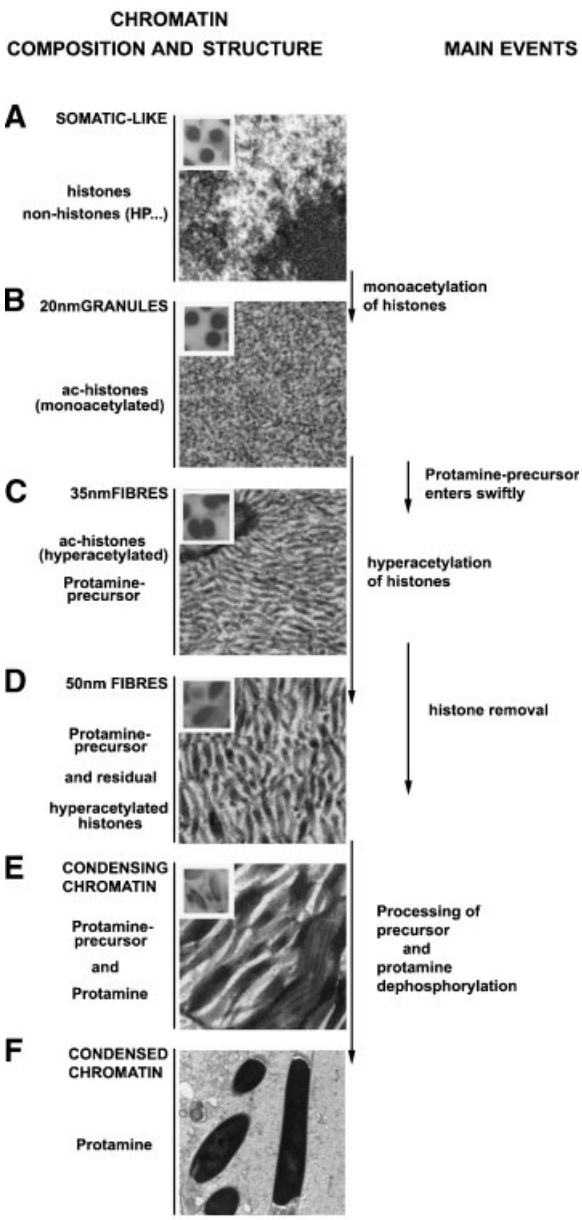

Fig. 8. Changes in chromatin condensation and in DNA-interacting proteins during *S. officinalis* spermiogenesis (from this work and from Martínez-Soler et al. [2007b]). Nuclei belonging to earliest spermatids (**A**) are spherical and contain somatic-like chromatin (eu- and heterochromatin). Histones from these spermatids display only basal levels of acetylation. First structural remodelling produces a chromatin organized into granules of 20 nm diameter, which are uniformly distributed in each round nucleus (**B**). Histone H4 is found mono-acetylated and the precursor-protamine has still not entered inside nuclei. This structural remodelling carries out without changes in the nuclear shape (inset). The second remodelling into fibres of 30–35 nm (**C**) develops simultaneously with the entrance of protamine-precursor to nuclei and with hyperacetylation of H4. This type of chromatin is found in nuclei that begin the elongation (inset). The third remodelling drives the formation of fibres of 40–50 nm in diameter and coincides with nuclear removal of histones. Remnants of H4 histone in this chromatin contain a high level of acetylation. Cell nuclear shape is elongated (inset). Condensation of chromatin in final phases (**E**,**F**) is given from progressive joining of 40–50 nm fibres. The mature sperm nucleus (F) is nearly cylindrical, 1 μm in diameter, with a length of 6 μm. Chromatin obtained from ripe sperm nuclei only contain non-phosphorylated protamine.

complete processing of the precursor molecule and protamine dephosphorylation.

The levels of histone acetylation in spermiogenesis depend on the equilibrium between activities of acetyl transferases and deacetylases [Hazzouri et al., 2000; Lahn et al., 2002], and has been found in all the cases studied. Nevertheless, until now the influence of histone acetylation over structural changes of spermiogenic chromatin has not been established. In this work we have found that during spermiogenesis of *S. officinalis* (model $H \rightarrow Pp \rightarrow P$), there are two structural changes of chromatin closely related with histone H4 acetylation: transition into 20 nm granules (shared by the majority of spermiogenesis) mainly correlated with a massive mono-acetylation of H4 K12, and transitions from 30–35 to 40–50 nm fibres, correlated with hyperacetylation and removal of nuclear histones.

ACKNOWLEDGMENTS

This work has been sponsored by a grant from Ministerio de Educación y Ciencia (Spain)-FEDER (grant BFU 2005-00123/BMC) and by a grant from the Natural Sciences and Engineering Research Council (NSERC) of Canada Grant OGP 0046399-02. Many thanks to Dr. Núria Cortadellas for her important assistance. Microscopic observations have been performed in "Serveis Científico-Tècnics de la Universitat de Barcelona"

REFERENCES

Calestagne-Morelli A, Ausió J. 2006. Long-range histone acetylation: Biological significance, structural implications, and mechanisms. Biochem Cell Biol 84:51–527.

Chiva M, Saperas N, Cáceres C, Ausió J. 1995. Nuclear basic proteins from the sperm of tunicates, cephalochordates, agnathans and fish. In: Jamieson BGM, Ausió J, Justine JL, editors. Advances in spermatozoal phylogeny and taxonomy Mem Mus Natn Hist Nat 166:501–514 Muséum National D'Histoire Naturelle Publications Scientifiques Diffusion, Paris, France.

Christensen ME, Rattner JB, Dixon GH. 1984. Hyperacetylation of histone H4 promotes decondensation prior to histone replacement of protamines during spermatogenesis in rainbow trout. Nucleic Acid Res 12:4575–4592.

Couppez M, Martin-Ponthieu A, Sautière P. 1987. Histone H4 from cuttlefish testis is sequentially acetylated. Comparison with acetylation of calf thymus histone H4. J Biol Chem 262:2854–2860.

Dimitrov SI, Wolffe AP. 1997. Fine resolution of histones by two dimensional polyacrylamide gel electrophoresis: Developmental implications. Methods: Companion Methods Enzymol 12:57–61.

Giménez-Bonafé P, Ribes E, Zamora MJ, Kasinsky HE, Chiva M. 2002. Evolution of octopod sperm. I. Comparison of nuclear morphogenesis in *Eledone* and *Octopus*. Mol Reprod Dev 62:363–367.

Harrison LG, Kasinsky HE, Ribes E, Chiva M. 2005. Possible mechanisms for early and intermediate stages of sperm chromatin condensation patterning involving phase separation dynamics. J Exp Zool 303A:76–92.

Hazzouri M, Pivot-Pajot C, Faure AK, Usson Y, Pelletier R, Sèle B, Khochbin S, Rousseaux S. 2000. Regulated hyperacetylation of core histones during mouse spermatogenesis: Involvement of histone-deacetylases. Eur J Cell Biol 79:950–960.

Johns EW. 1967. A method for the selective extraction of histone fractions f2(a1) and f2(a2) from calf thymus deoxyribonucleoprotein at pH 7. Biochem J 105:611–614.

Lahn B, Zhao LT, Zhou J, Barndt R, Parvinen M, Allis CD, Page D. 2002. Previously uncharacterized histone acetyltransferases implicated in mammalian spermatogenesis. Proc Natl Acad Sci 99:8707–8712.

Lewis J, Song Y, deJomg M, Bagha S, Ausió J. 2003. A walk through vertebrate and invertebrate protamines. Chromosoma 111:473–482.

Lewis J, Saperas N, Song Y, Zamora MJ, Chiva M, Ausió J. 2004. Histone H1 and the origin of protamines. Proc Natl Acad Sci USA 101:4148–4152.

Martínez-Soler F, Kurtz K, Chiva M. 2007a. Sperm nucleomorphogenesis in the cephalopod *Sepia officinalis*. Tissue Cell doi:10.1016/j.tice.2007.01.005.

Martínez-Soler F, Kurtz K, Ausió J, Chiva M. 2007b. Transition of nuclear proteins and chromatin structure in spermiogenesis of *Sepia officinalis*. Mol Reprod Develop 74:360–370.

Martin-Ponthieu A, Wouters-Tyrou D, Belaiche D, Sautière P, Schindler P, van Dorsselaer A. 1991. Cuttlefish sperm protamines. 1. Amino acid sequences of two variants. Eur J Biochem 195:611–619.

Oliva R, Dixon GH. 1991. Vertebrate protamine genes and the histone-to-protamine replacement reaction. Prog Nucleic Acid Res Mol Biol 40:25–94.

Saperas N, Ribes E, Buesa C, García-Hegart F, Chiva M. 1993. Differences in chromatin condensation during spermiogenesis in two species of fish with distinct protamines. J Exp Zool 265:185–194.

Saperas N, Chiva M, Casas MT, Campos L, Eirín-Lopez A, Frehlick LJ, Prieto C, Subirana JA, Ausió J. 2006. A unique vertebrate histone H1-related protamine-like protein results in an unusual sperm chromatin organization. FEBS J 273:4548–4561.

Subirana JA. 1983. Nuclear proteins in spermatozoa and their interactions with DNA. In: André J, editor. . The sperm Cell. The Hague: Martinus Nijhoff. pp 117–124.

Wouters-Tyrou D, Chartier-Harlin MC, Martin-Ponthieu A, Boutillon C, van Dorsselaer A, Sautière P. 1991. Cuttlefish spermatid-specific protein T. Molecular characterization of two variants T1 and T2, putative precursors of sperm protamine variants Sp1 and Sp2. J Biol Chem 266:17388–17395.